



THE UNIVERSITY *of* EDINBURGH

Edinburgh Research Explorer

Petroleum emplacement inhibits quartz cementation and feldspar dissolution in a deeply buried sandstone

Citation for published version:

Xia, C, Wilkinson, M & Haszeldine, S 2020, 'Petroleum emplacement inhibits quartz cementation and feldspar dissolution in a deeply buried sandstone', *Marine and Petroleum Geology*, pp. 104449. <https://doi.org/10.1016/j.marpetgeo.2020.104449>

Digital Object Identifier (DOI):

[10.1016/j.marpetgeo.2020.104449](https://doi.org/10.1016/j.marpetgeo.2020.104449)

Link:

[Link to publication record in Edinburgh Research Explorer](#)

Document Version:

Peer reviewed version

Published In:

Marine and Petroleum Geology

General rights

Copyright for the publications made accessible via the Edinburgh Research Explorer is retained by the author(s) and / or other copyright owners and it is a condition of accessing these publications that users recognise and abide by the legal requirements associated with these rights.

Take down policy

The University of Edinburgh has made every reasonable effort to ensure that Edinburgh Research Explorer content complies with UK legislation. If you believe that the public display of this file breaches copyright please contact openaccess@ed.ac.uk providing details, and we will remove access to the work immediately and investigate your claim.



1 Petroleum emplacement inhibits quartz cementation and feldspar
2 dissolution in a deeply buried sandstone

3 **Changyou Xia^{1,2}, Mark Wilkinson^{1,*} and Stuart Haszeldine¹**

4 *¹School of GeoSciences, University of Edinburgh, Grant Institute, James Hutton Road,*
5 *Edinburgh, EH9 3FE, UK*

6 *²Shenzhen Research Center on Climate Change, School of Economics and Management, Harbin*
7 *Institute of Technology (Shenzhen), Shenzhen, 518055, China*

8

9 Corresponding author: Mark Wilkinson, mark.wilkinson@ed.ac.uk

10

11 **ABSTRACT**

12 Whether the emplacement of petroleum in sandstone reservoirs can preserve porosity during burial
13 remains controversial. In the Kessog Field, UK Central North Sea, average porosities of the crestal
14 sections of the fluvial-deltaic Pentland Formation reservoir can exceed 25 % despite burial to 4
15 km or more. The predicted porosity for the reservoir at this depth is only around 14 % based on
16 regional data. Oil saturation data, thin-section point counts, grain-size and sorting measurements,
17 reservoir pressure, and SEM images were combined to analyze the cause of the high reservoir
18 porosity. Petroleum emplacement preventing cementation is the most likely mechanism for
19 porosity preservation. Facies variation is not responsible, as the high-porosity sandstones from the
20 crestal well are, in terms of average grain-size (fine-grained) and sorting coefficient (moderately
21 well-sorted), nearly the same as the lower porosity sandstones from the flanks of the field (average
22 porosity 13 - 15%). Other potential porosity-preservation mechanisms, such as overpressure,

23 grain-coats and feldspar dissolution can be discounted. The sandstones with high oil saturations
24 are characterized by: 1) most porosity being primary as opposed to secondary; 2) there being 2 –
25 5 % less quartz cement than in the water-saturated sandstones; 3) there being 2 – 3 % more K-
26 feldspar and 2 – 6 % less kaolin than the water-saturated counterparts. This study demonstrates
27 that petroleum emplacement can effectively inhibit quartz cementation and K-feldspar
28 transformation to kaolin in sandstone reservoirs.

29

30 **Keywords:** quartz cementation, K-feldspar dissolution, reservoir quality, porosity preservation,
31 sandstone porosity

32

33 **INTRODUCTION**

34 Petroleum emplacement in sandstone reservoirs can potentially preserve reservoir porosity
35 by inhibiting quartz cementation and other diagenetic processes. This is one potential mechanism
36 that may form deep, high-porosity oil and gas reservoirs (Bloch et al., 2002; Worden et al., 1998).
37 However, this proposition is highly contentious. Some studies have recorded higher porosity and
38 less quartz cement in the reservoirs where pore waters have been replaced by petroleum, thereby
39 invoking petroleum emplacement as a mechanism of porosity preservation (e.g. Gluyas et al.,
40 1993; Marchand et al., 2001; Worden et al., 2018; Lei et al., 2019). Nevertheless, at least an equal
41 number of studies have reached the opposite conclusion; these studies observed on-going quartz
42 cementation in oil-filled reservoirs and that the porosity of these reservoirs does not appear to be
43 higher than the water-filled counterparts. Hence, they conclude that petroleum does not affect
44 reservoir porosity (e.g. Giles et al., 1992; Barclay and Worden, 1998; Midtbø et al., 2000;
45 Molenaar et al., 2008; Taylor et al., 2010).

46 Understanding the effect of petroleum on sandstone porosity has great scientific and
47 commercial significance. Firstly, this can help to develop a more accurate predictive model for
48 reservoir porosity. Second, if petroleum is capable of preserving porosity, it means the porosity of
49 petroleum reservoirs can be maintained at great depths (e.g. >5000 m) once petroleum is emplaced.
50 As a result, the lower depth limit of exploration targets can be extended to a deeper regime, and
51 the number of high-quality deep reservoirs may be more significant than previous estimates.
52 Moreover, this knowledge is also of great importance for oilfield production, as it provides the
53 possibility of predicting the distribution pattern of porosity-permeability within an oilfield by
54 modelling the history of petroleum filling, reducing the need to collect expensive core data
55 (Worden et al., 1998).

56 However, assessing the effect of petroleum on sandstone porosity is often difficult. In addition
57 to petroleum emplacement, there are other factors that may also help preserve porosity, such as
58 reservoir overpressure and grain coats (Oye et al., 2018; Storvoll et al., 2002). For a high-porosity
59 sandstone, it is usually difficult to discern and quantify the amount of porosity preserved by each
60 of the factors (Aase and Walderhaug, 2005; Wilkinson and Haszeldine, 2011). However, if there
61 is a case where the effect of other porosity-preservation mechanisms, except for petroleum
62 emplacement, can be shown to be minimal, then demonstrating the porosity-preservation effect of
63 petroleum emplacement might be possible. The reservoir sandstones of the Kessog Field in the
64 North Sea (Figure 1) exhibit porosities up to 11% higher than the predicted porosity for the burial
65 depth (Figure 2A), and most of these high-porosity sandstones are also characterized by high oil
66 saturation ($S_o > 40\%$; Figure 2B), which indicates that high porosity and high oil saturation are
67 possibly related. This paper aims to address two questions: are the high-porosity sandstones of the
68 Kessog Field the result of high oil saturation? And what are the porosity and petrographic

69 characteristics of the high-porosity sandstones potentially affected by petroleum emplacement?
70 Petrographic data, conventional core data, well log data and reservoir structure data are utilized to
71 test the hypothesis that the preservation of the high porosity in the Kessog Field is related to
72 petroleum emplacement.

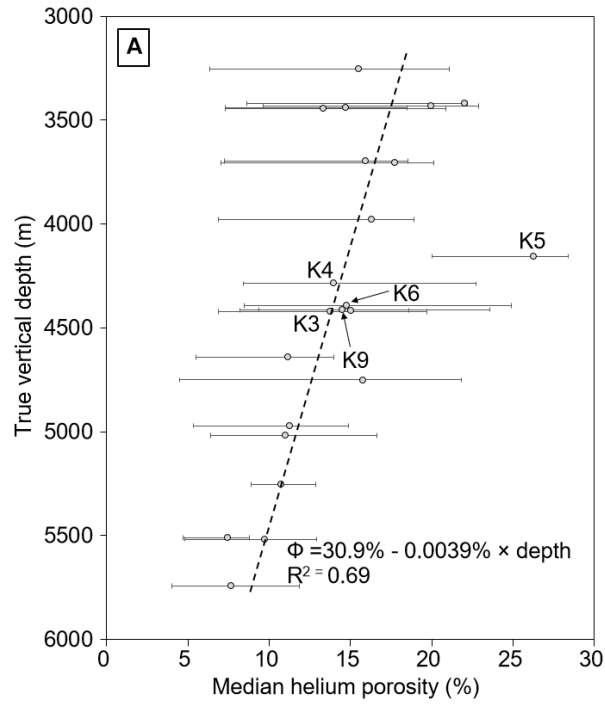
73



74

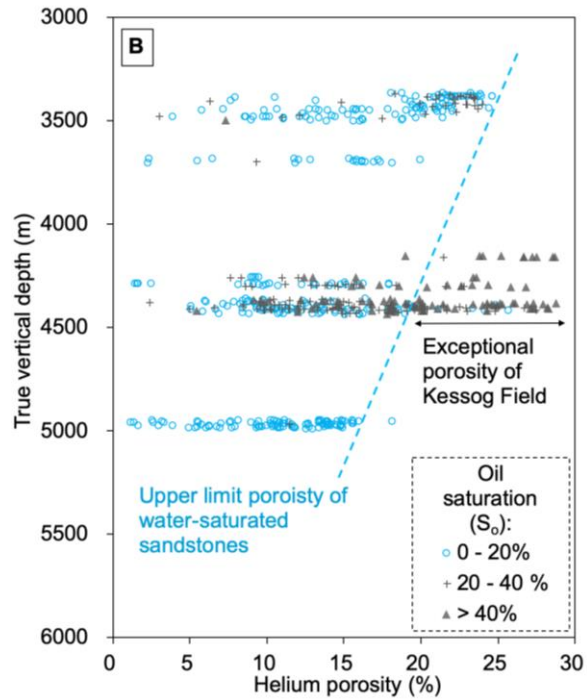
75

Figure 1. Location of the Kessog Field in the North Sea



76

77



78

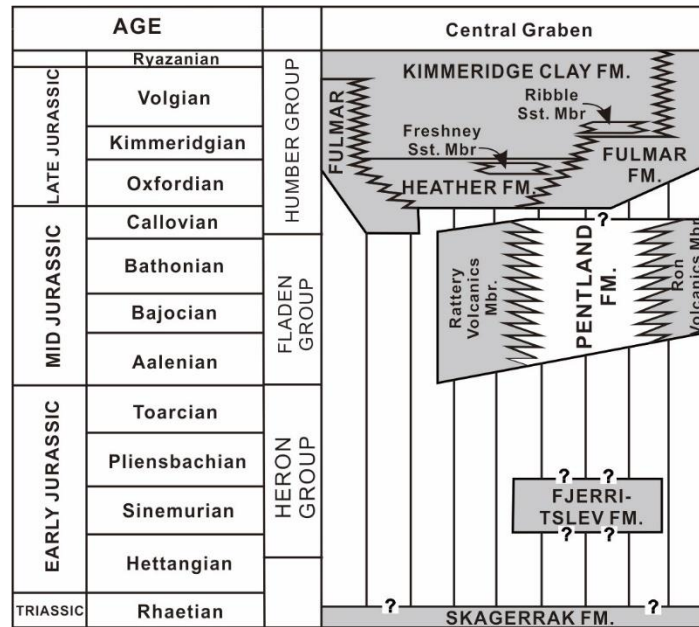
79 Figure 2. (A) Median porosity (P50) of different wells drilled the Pentland Sandstone (Error bar =

80 P10 to P90 range of the porosity). The porosity data come from 22 Pentland wells with 2372

81 porosity measurements (summary in Supplementary Data). Wells K3, K4, K5, K6 and K9 are
 82 located in the Kessog Field. Median porosity of well K5, which is drilled at the crest of the field
 83 structure, is 11% higher than the empirical prediction. (B) High porosity of petroleum-saturated
 84 sandstones at the Kessog Field. The sandstones buried at 4.1-4.5 km are from wells K3, K4, K5
 85 and K6. Sandstones at 3.3-3.7 km and 4.8-5.0 km are from other six Pentland wells where
 86 petroleum saturation data are available (Supplementary Data).

87

88 **GEOLOGICAL SETTING**



89

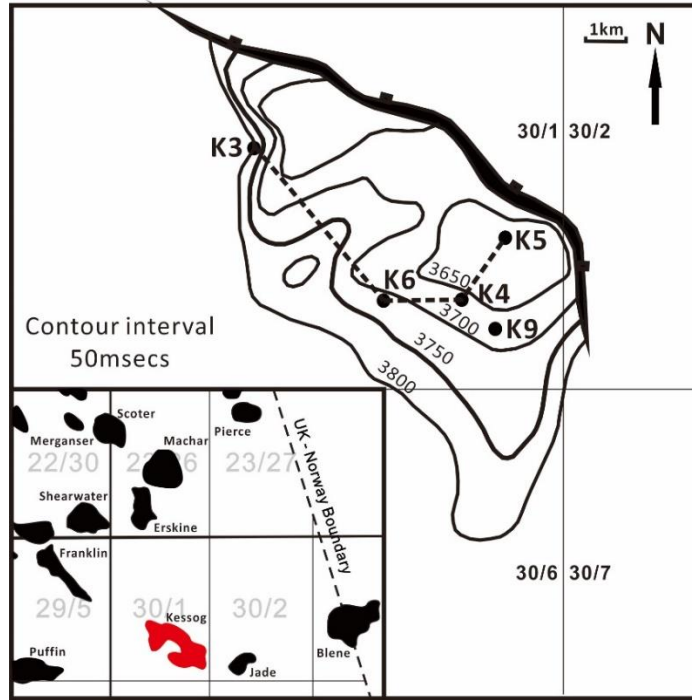
90 Figure 3. Stratigraphic position of the Pentland Formation within the Jurassic strata of the Central
 91 Graben (adapted from Richards et al., 1993). The Pentland Formation lies unconformably between
 92 the sediments of Upper Jurassic Humber Group and the Triassic Skagerrak Formation.

93 The term ‘Pentland Formation’ was initially introduced by Deegan and Scull (1977) to
 94 represent a heterolithic unit of sandstone, siltstone, shale and coal that lies between the Upper
 95 Jurassic marine sediments of the Humber Group and the Triassic non-marine sediments of the

96 Skagerrak Formation in the Central North Sea (Figure 3). Sediments of the Pentland Formation
97 are predominantly sandstones with interbedded shales and coals deposited in a fluvial-deltaic or
98 lagoonal environment on a coastal plain (Clark et al., 1993; Deegan and Scull, 1977). The
99 formation is widespread in the Central North Sea, but for most oilfields, it is only a minor reservoir
100 (Eriksen et al., 2003). Reserves in the reservoirs of the Pentland Formation are usually much
101 smaller than in the Fulmar or Skagerrak Formation (Gluyas and Hichens, 2003). The Kessog Field,
102 however, is an exception, for which the principal reservoir is the Pentland Formation.

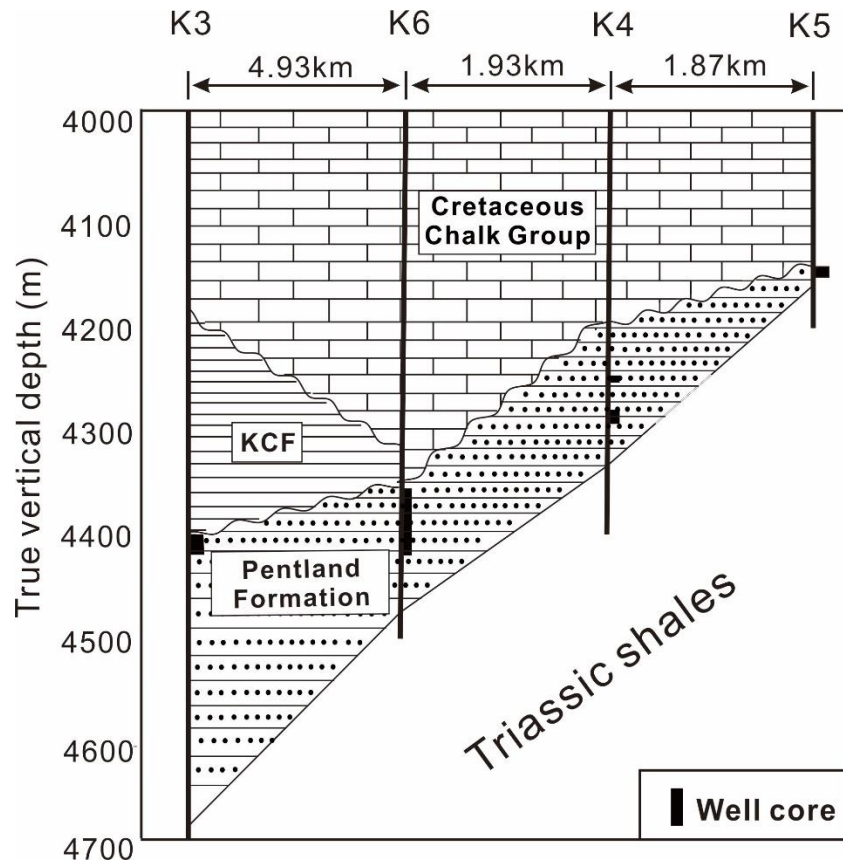
103 The Kessog Field is a high-pressure, high-temperature gas condensate field discovered by BP
104 in 1985. The reserves are equivalent to 100 million barrels of oil (Offshore Europe, 2001).
105 Developing the field, however, is a great technical challenge due to a combination of extreme
106 pressures and temperatures and a complex, compartmentalized reservoir.

107 The field is a tilted fault block bounded by a NW-SE trending fault on the NE side (Figure 4
108 and Figure 5). The western part of the field is sealed by shales, where the Pentland Formation is
109 unconformably overlain by the Upper Jurassic Kimmeridge Clay Formation (Figure 5). In
110 comparison, the eastern part is sealed by Cretaceous carbonate sediments, possibly because the
111 Kimmeridgian shales have been eroded during the Late Jurassic or Early Cretaceous. The
112 petroleum source for the field is most likely the Kimmeridge Clay Formation.



113

114 Figure 4. Structural map of the Kessog Field. The Kessog Field is a half-graben structure. The
 115 dashed line represents the cross-section in Figure 5.



116

117 Figure 5. A cross-section across the Kessog Field based on the logs of wells K3, K4, K5 and K6.

118 Note the distances between the wells are unequal. KCF = Kimmeridge Clay Formation

119

120 METHODS

121 There are five wells in the Kessog Field for study: wells 30/1c -3, -4, -5, -6 & -9, which are
 122 labelled as K3, K4, K5, K6 and K9 in this paper. Helium porosity, petroleum saturation, well log
 123 and formation test data of the wells penetrated the Pentland Formation are accessible in the UK
 124 Common Data Access (CDA) database. The sandstone porosity is measured using the Gas
 125 Expansion Method: a known volume of helium gas at a known pressure was expanded into a
 126 chamber containing a core plug sample in a Boyle's Law porosimeter, whereby the grain volume
 127 in the samples can be measured. Then, the bulk volume of the sample was calculated by mercury

128 displacement using a hand-operated mercury displacement pump at atmospheric pressure. The
129 porosity is determined by dividing the grain volume to the bulk volume of the sample. The oil
130 saturation values were determined using the Retort Method. This method first injects mercury into
131 the gas filled pore of a sample using a mercury pump, where the injected volume of mercury is
132 equivalent to the volume of gas. Then, the method requires to heat the sample and measure the
133 volumes of water and oil driven off. The oil saturation value is the ratio of the volume of oil to the
134 total pore volume, which is the sum of the volumes of oil, gas and water. The reservoir temperature
135 and pressure information were obtained from temperature log and repeated formation test results.
136 These analyses were conducted by professional third-party core laboratories using established
137 analytical methods, and the data are therefore considered to be reliable.

138 Thirty-nine sandstone samples from the borehole cores of the five wells of the Kessog Field
139 (6-8 samples per well) were collected from the UK National Core Collection of British Geological
140 Survey for study. The reservoir sandstones were evenly sampled across the reservoir sections
141 consisting of sandstones, while the shale and coal sections were avoided. Samples were then
142 impregnated with blue resin, made into thin-sections and point-counted (250 counts/slide) for
143 mineralogical composition and porosity. Additionally, point-count data of 68 Kessog Field
144 sandstone samples from Wilkinson et al. (2014) were also used.

145 Grain size was determined by calculating the mean diameter of 100 quartz grains per sample
146 on microphotographs. Since this mean grain size is measured on a 2D cross-section of quartz
147 grains, the conversion into the actual 3D mean grain size is performed by multiplying the 2D grain
148 size with a factor of 1.273 (Kong et al., 2005). Sorting was based on the grain size data: the data
149 were converted from metric to the phi-scale, then the 5th, 16th, 84th and 95th percentiles of the

150 phi-based grain size distribution were used to compute the sorting coefficient using Eq. (1)
151 (McManus, 1988).

$$152 \quad \text{Sorting coefficient} = (\Phi_{84} - \Phi_{16})/4 + (\Phi_{95} - \Phi_5)/6.6 \quad (1)$$

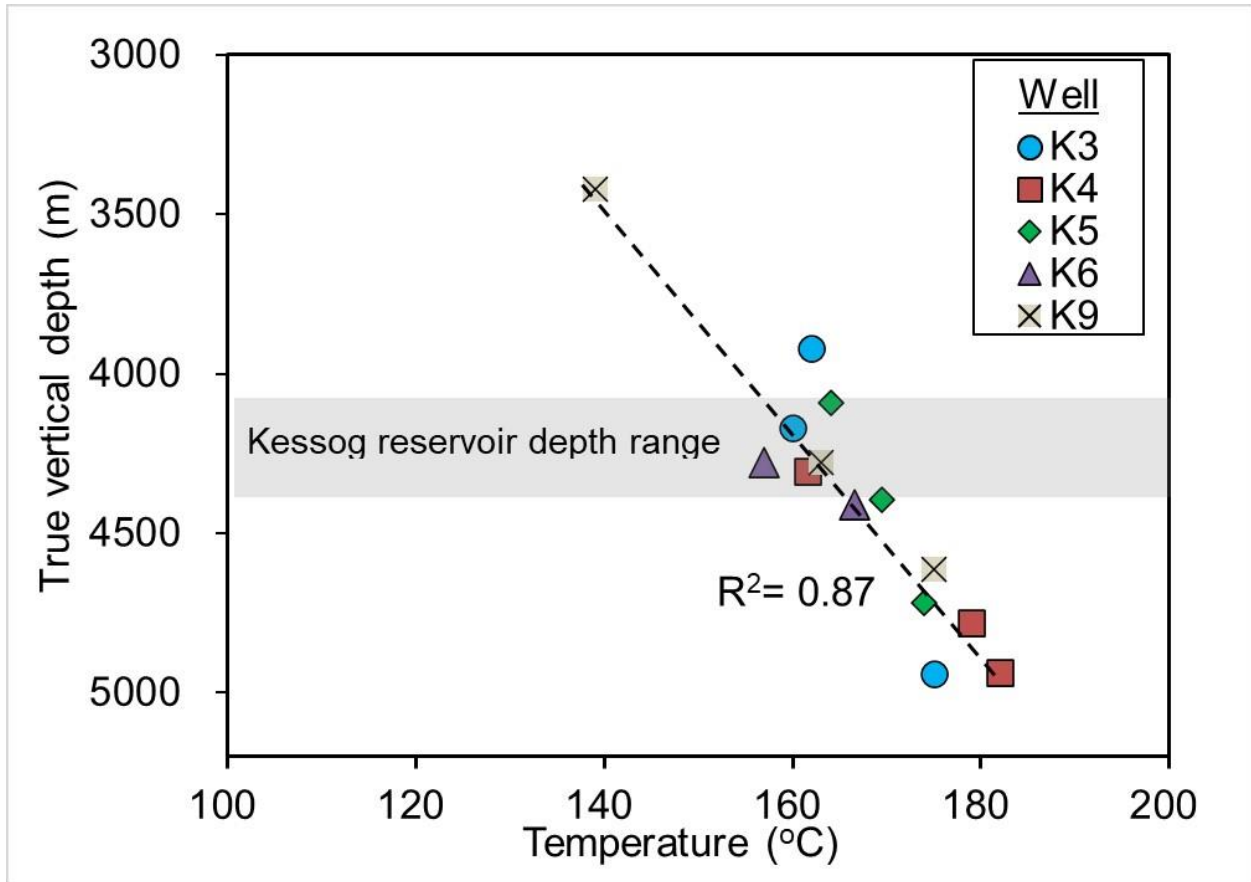
153 To observe the grain-coats and cement on grain surfaces, we selected two samples from each
154 of the five wells in the Kessog Field, for secondary electron imaging under a Zeiss SIGMA
155 scanning electron microscope (SEM) at an accelerating voltage of 20 kV. Samples with fresh
156 fractures were coated with platinum and stub-mounted for examination in the SEM. All the
157 experimental studies were completed in the laboratories of the School of Geosciences, University
158 of Edinburgh.

159

160 **RESULTS**

161 **Reservoir temperature and pressure**

162 The Kessog Field reservoir is currently at a depth of 4.1 – 4.5 km. Between 170-70 Ma, the
163 reservoir was buried to only shallow depths (<1000 m), and from 70 Ma to present, the reservoir
164 experienced rapid burial to a depth below 4.1 km. The temperature in the reservoir is currently
165 around 160-170°C
166 (



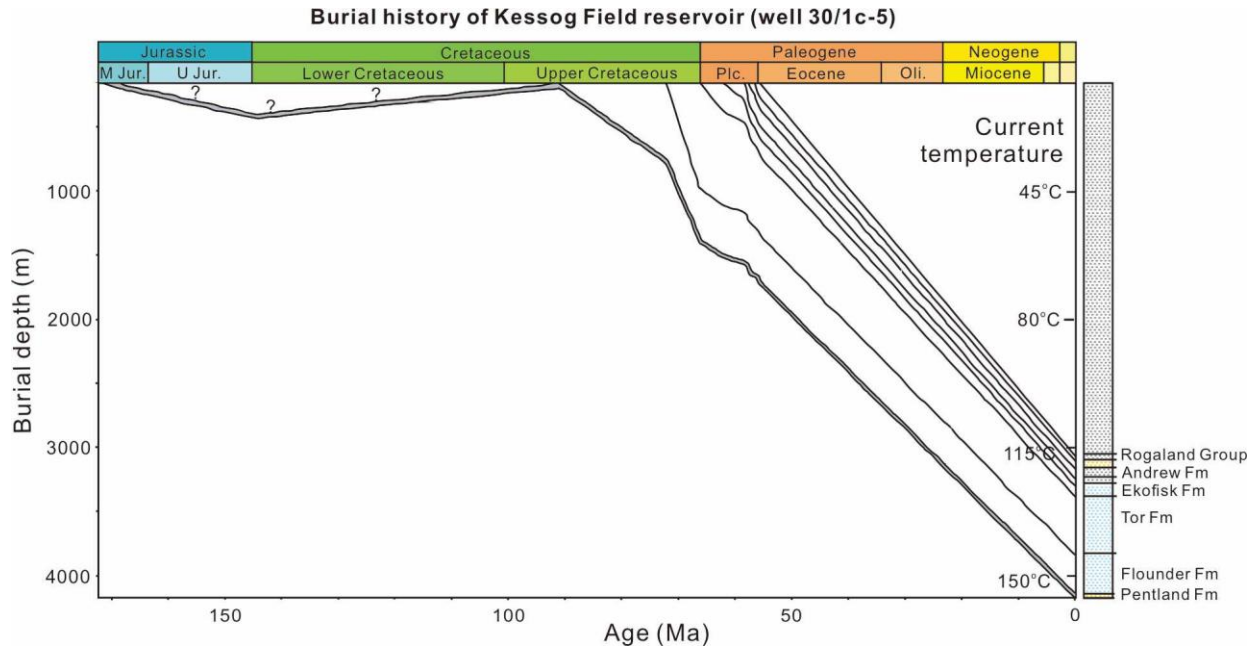
167

168 Figure 7). The Pentland Formation is highly overpressured below the depth of 4.1 km (Figure 8).

169 The degree of overpressure in the Kessog Field is close to the other deep Pentland reservoirs, with

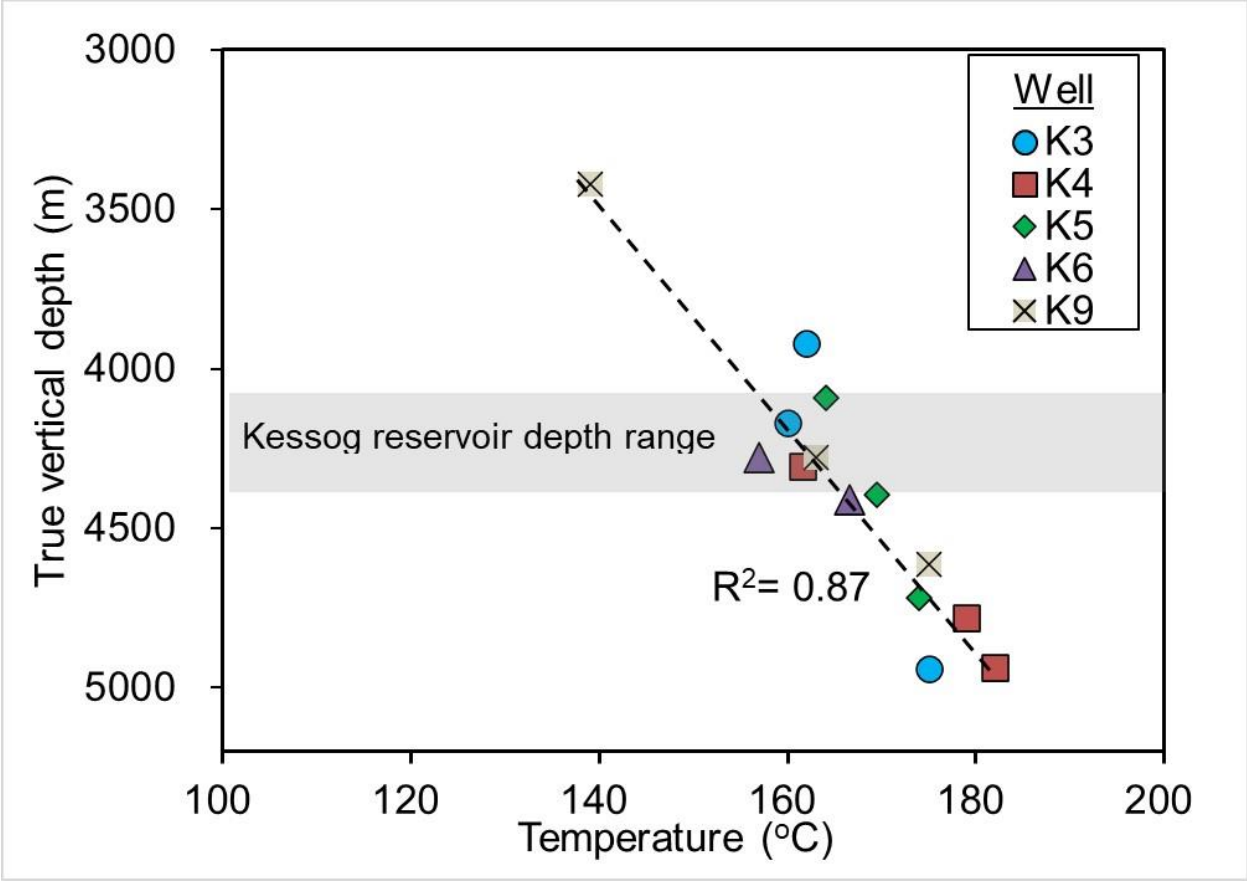
170 reservoir pressure approaching the lithostatic pressure.

171



172

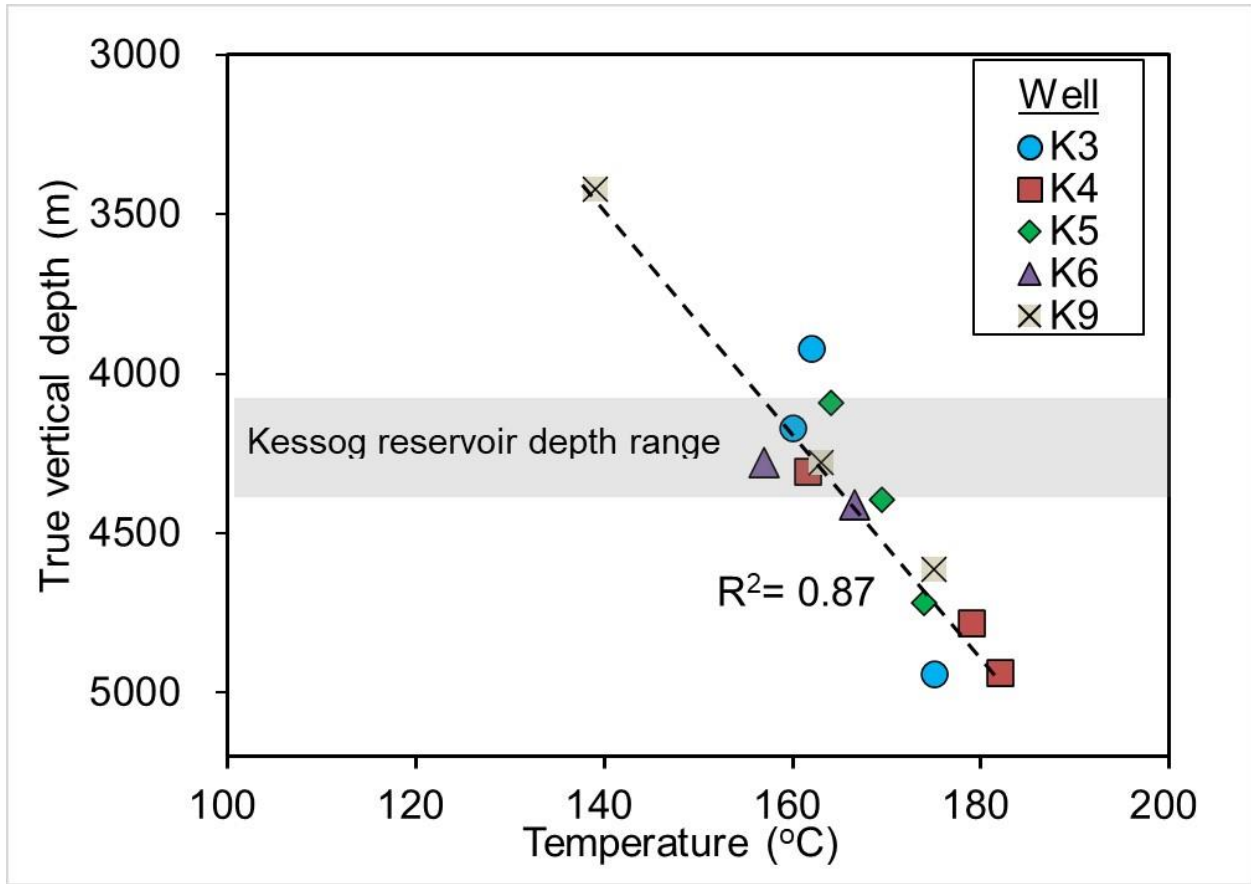
173 Figure 6. Burial curve for the Kessog Field from well K5. The burial process was modelled using
 174 PetroMod™ software. The thickness of the sediments eroded during the Early Cretaceous is
 175 uncertain. The Cenozoic sediments lack a clear stratigraphy, and hence burial has been assumed
 176 to be at a constant rate. The surface temperature and geothermal gradient are assumed to be 10°C
 177 and 35°C/km (see



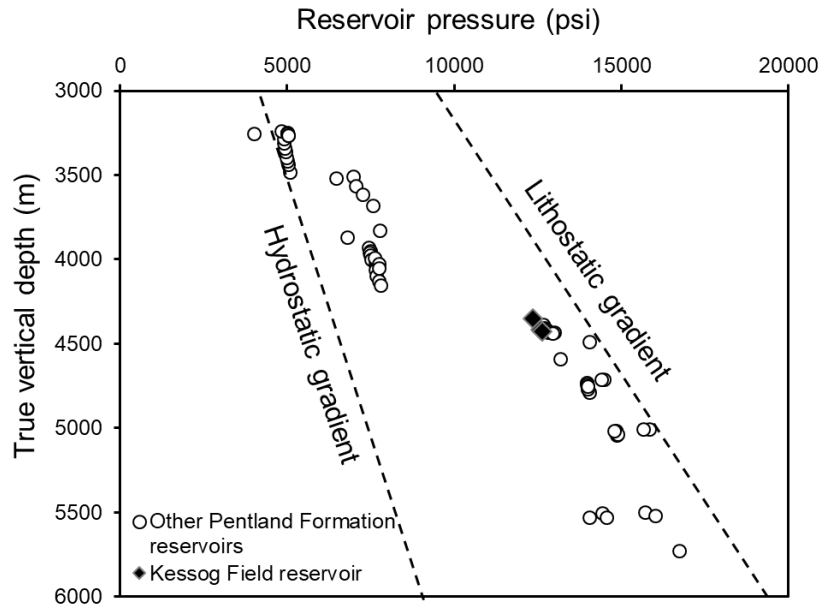
178

179 Figure 7).

180



181
 182 Figure 7. Subsurface temperature increase near the Kessog Field. The data are corrected log
 183 temperatures. The geothermal gradient is around 35°C/km.



185 Figure 8. Reservoir pressure of the Pentland Formation versus depth. The Kessog Field is highly
186 overpressured as with other deep Pentland reservoirs below 4.2 km. The hydrostatic and lithostatic
187 gradients are from Moss et al. (2003). The pressure data are from 11 Pentland wells.

188

189 Porosity and petrography

190 The average helium porosity of well K5 is abnormally high at 25% (Table 1 and
191 Supplementary Data), whereas for the depth of the Kessog Field, only 14 % would be predicted
192 from regional Pentland Formation data (Figure 2A). In contrast, the average porosities of wells K3,
193 K4, K6 and K9 are significantly lower (Table 1), but are consistent with the regional mean porosity
194 (Figure 2A). However, it is notable that a few sandstones of wells K3, K4 and K6 are also of high
195 porosity, comparable to well K5, and the majority of these are characterized by high oil saturation
196 ($S_o > 40\%$, Figure 2B).

197

198 Table 1. Average porosity and oil saturation (S_o) of Kessog Field wells (in order of increasing
199 depth)

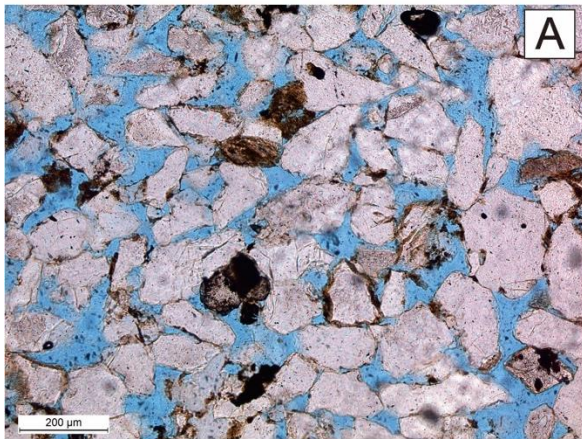
Well	Avg. TVD (m)	Avg. helium porosity (%)	Avg. oil saturation (%)	Reservoir thickness (m)
K5	4155	24.7±1.1	57±6	23.5
K4	4288	14.1±0.7	27±2	138
K6	4392	15.8±0.5	35±1	117.5
K9	4412	15.2±0.7	n.a	203
K3	4423	13.7±0.5	14±1	280

Note: mean values of helium porosity and oil saturation are expressed as ± 1 standard error of the mean.

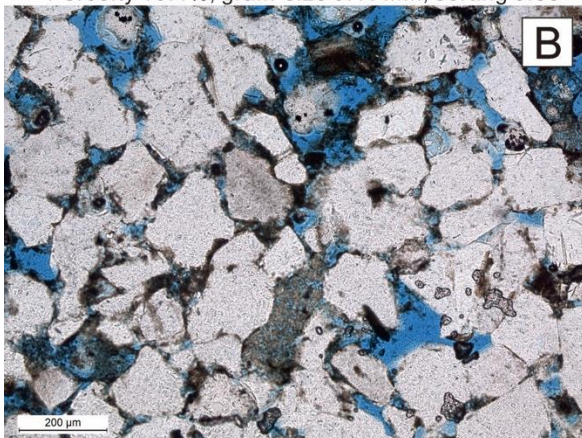
200

201 Photomicrographs of typical reservoir sandstones from well K5, K4, K3 and K9 are illustrated
202 in Figure 9, showing that the porosity of these sandstones generally decreases with depth. The

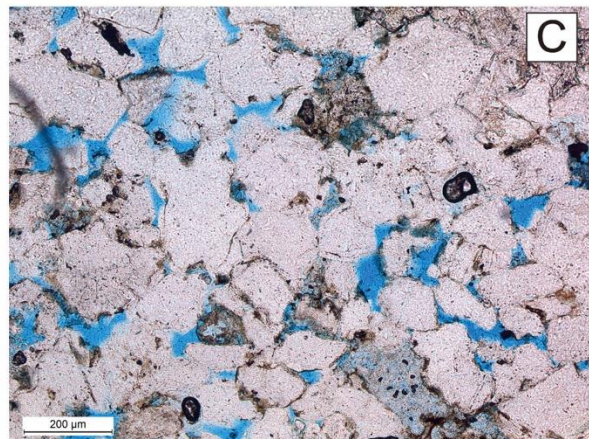
203 petrographic data suggest that the average sandstone grain size (corrected to 3D) of different wells
204 are nearly uniform, lying within the range of 0.14 - 0.17 mm (Table 2). The sandstones also exhibit
205 similar degrees of sorting, with sorting coefficients within the range of 0.54-0.63 (moderately well-
206 sorted sand, Table 2); the sandstones of well K4 are slightly less well sorted (sorting coefficient:
207 0.77), so are moderately sorted sands. Grain contacts in the high-porosity sandstones are typically
208 long contacts (Figure 10), whereas in the less porous and more quartz-cemented sandstones,
209 concave-convex (CC) contacts are common, indicating a higher degree of chemical compaction in
210 the latter.



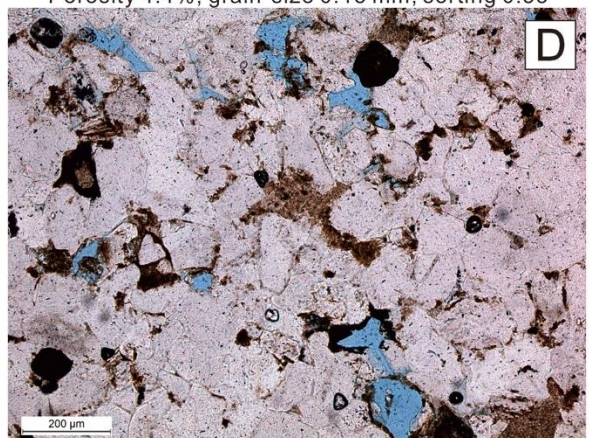
Well K5, 4185 m,
Porosity 10.4%, grain-size 0.11 mm, sorting 0.58



Well K4, 4327.68 m,
Porosity 7.6%, grain-size 0.15 mm, sorting 0.70

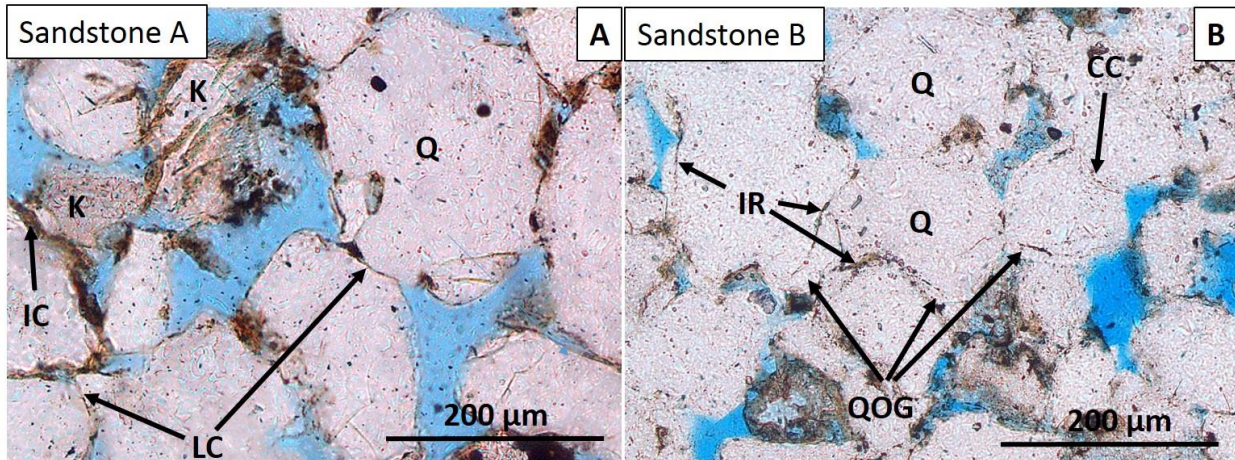


Well K3, 4435.55 m,
Porosity 4.4%, grain-size 0.15 mm, sorting 0.53



Well K9, 4444.72 m,
Porosity 3.6%, grain-size 0.11 mm, sorting 0.57

212 Figure 9. Microphotographs showing sandstones in different Kessog wells (increasing depth from
213 A to D). The sandstones are very fine to fine-grained with similar degrees of sorting, and all the
214 photos are on the same scale. In the shallowest well K5, the sandstones are porous; whereas in the
215 deepest well K9, the sandstones are highly cemented.



216
217 Figure 10. (A) Microphotograph of a high-porosity sandstone from the well K5 (TVD 4159 m,
218 point-counted porosity 10.4%, avg. grain size 0.11 mm, sorting 0.58). (B) a sandstone from well
219 K3 with similar grain size and sorting as in (A) (TVD 4410.55 m, point-counted porosity 4.4%,
220 avg. grain size 0.15 mm, sorting 0.53). The most common grain contact type in sandstone A is
221 long contact (LC), whereas in sandstone B, concave-convex (CC) contact is common, indicating
222 a higher degree of chemical compaction. Thick illite coats (IC) only appear on the surface of a
223 small number of quartz grains. Illite rims (IR), as shown in (B), commonly fail to prevent quartz
224 overgrowth. Q = detrital quartz grains; QOG = quartz overgrowth; K = K-feldspar.

225 The framework grains of the Pentland Sandstone in the Kessog Field are dominated by detrital
226 quartz (Table 2 and Supplementary Data). Optically-identifiable feldspar in most cases is present
227 in only small amounts (<4%), and lithic fragments are nearly absent, hence the sandstones are
228 quartz arenites (Folk, 1974), in line with the regional norm (Wilkinson et al., 2014). The principal

229 clay minerals are kaolin (0.7 - 5.5%) and illite (8 – 17%; Table 2). The kaolin in the sandstones
230 occurs in the form of dense blocky and vermicular aggregates, which fill oversized pores left
231 presumably by the dissolution of feldspar grains. The morphology of illite is more diverse: it can
232 be compacted clasts, grain rims or coats, matrix in-filling primary porosity or very occasionally a
233 replacement of kaolin. The majority of illite occurs as compacted clasts, which are considered to
234 be detrital in origin. The volume of K-feldspar shows a decreasing trend with depth: from $3.8 \pm 0.4\%$
235 from well K5 to $1.3 \pm 0.3\%$ in K3 and $0.6 \pm 0.3\%$ in K9 (Table 2). Meanwhile, kaolin increases from
236 $0.7 \pm 0.2\%$ (well K5) to $5.5 \pm 1.0\%$ (well K3) and 6.3 ± 1.7 (well K9).

237 Quartz overgrowth (QOG) is the dominant cement in the sandstone reservoirs of the Kessog
238 Field. The average volume of quartz overgrowth determined by point-counting is least in the
239 crestal well K5 ($2.8 \pm 0.4\%$, Table 2); in deeper wells the average volume increases to $6.4 \pm 1.0\%$
240 in well K3 and $7.8 \pm 2.2\%$ in well K9 (Table 2, Figure 11). Under SEM, some quartz cement in
241 the high-porosity sandstones is present as an unusual, anhedral form (Figure 12A), in contrast to
242 the euhedral, smooth crystal faces of standard quartz cement (Figure 12B). The SEM analysis was
243 performed on two sandstone samples per well. The irregular outlines of the cement are common
244 in the sandstones of well K5, and occasionally observed in well K3. In the sandstones of other
245 wells, however, quartz cement appears as standard, euhedral crystals.

246 The sandstones of the crestal well (K5) contain mostly primary porosity ($10.3 \pm 0.9\%$, **Error!**
247 **Reference source not found.**), and secondary porosity is of lesser importance ($3.9 \pm 0.5\%$). In
248 the other wells, primary porosity typically varies between 1 and 5 %, and secondary porosity
249 between 2 and 5 % (Table 2). From the relics of dissolved minerals, it can be inferred that the
250 secondary porosity was created mostly by the dissolution of feldspar grains. Primary porosity
251 hence appears to be important for the reservoir quality of the Kessog Sandstone. Figure 13A shows

252 that primary porosity has a positive correlation with the point-counted total porosity. In the
 253 sandstones of high porosity, the porosity is predominantly primary porosity (Figure 13A). In
 254 contrast, the percentage of secondary porosity is widely scattered in high-porosity sandstones, with
 255 no correlation with the amount of point-counted total porosity (Figure 13B).

256

257 Table 2. Average composition, grain-size and sorting of the sandstones

Well	n*	Quartz (%)	K-feldspar (%)	QOG [†] (%)	Illite** (%)	Kaolin (%)	Primary porosity (%)	Secondary porosity (%)	Grain-size (mm)	Sorting
K5	28	62±1	3.8±0.4	2.8±0.4	9.2±1.2	0.7±0.2	10.3±0.9	3.9±0.5	0.14±0.01	0.58±0.02
K4	13	60±1	1.8±0.3	4.0±0.9	17.0±3.0	2.9±0.6	3.7±1.1	5.0±0.8	0.17±0.01	0.71±0.04
K6	50	54±1	0.6±0.1	6.4±0.6	14.7±1.9	4.8±0.5	5.5±0.7	3.1±0.3	0.15±0.01	0.57±0.02
K9	8	65±1	0.6±0.3	7.8±2.2	11.8±2.6	6.3±1.7	1.3±0.6	3.2±1.3	0.15±0.02	0.63±0.05
K3	8	68±2	1.3±0.3	6.4±1.0	8.2±1.9	5.5±1.0	2.0±0.7	2.1±0.5	0.15±0.01	0.54±0.04
Avg. PF [§]	245	60.6	1.4	6.9	11.4	4.0	4.1	3.3	n.a	n.a

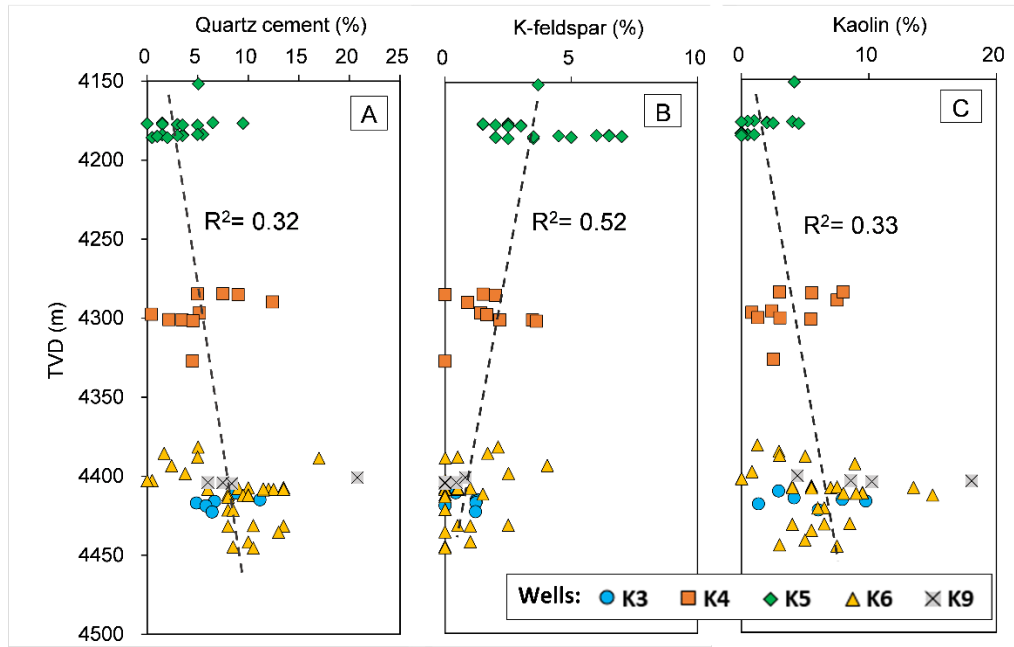
Note: mean values are expressed as ± 1 standard error of the mean. See Supplementary Data.

*n = number of samples;

** The illites are compacted clasts that are interpreted to be detrital in origin. Grain-coating illite or the illite replacing kaolin occur very occasionally in the reservoir and their volumes are below the resolution of the point-count method.

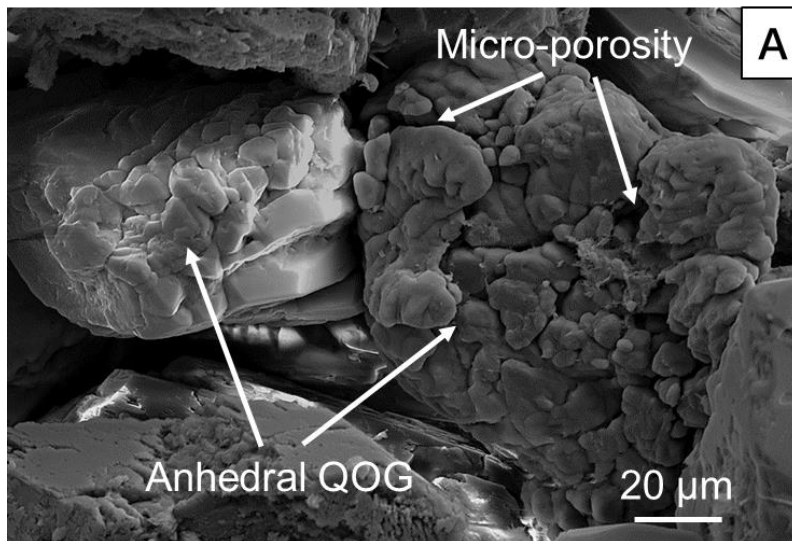
†QOG = quartz overgrowth;

§Avg. PF = average composition of the Pentland Sandstone buried at 3000-6000 m, data from Wilkinson et al. (2014).

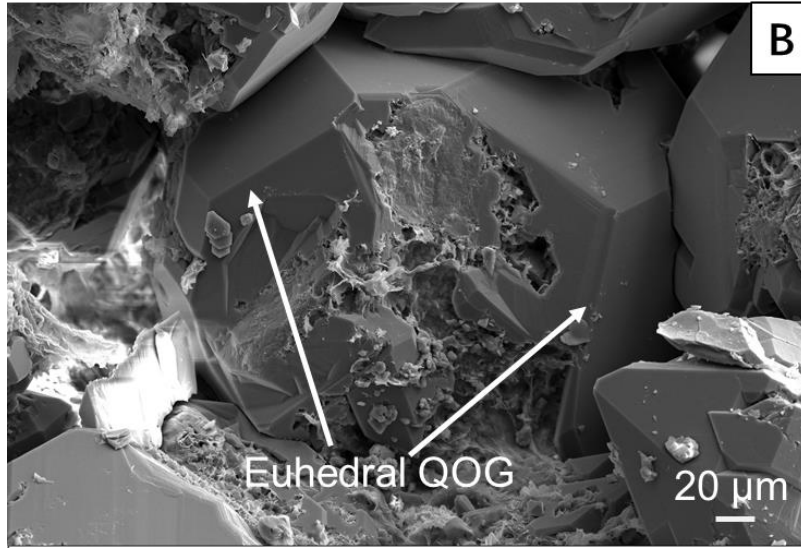


258

259 Figure 11. Variation of point-counted (A) quartz cement, (B) K-feldspar and (C) Kaolin with depth
 260 in the main sandstone facies (fine-grained) of Kessog Field reservoir. Siltstone, very fine-grained
 261 and medium-grained sandstone samples were excluded in these figures. The amount of quartz
 262 cement and kaolin increase, with depth while K-feldspar shows a decreasing trend.

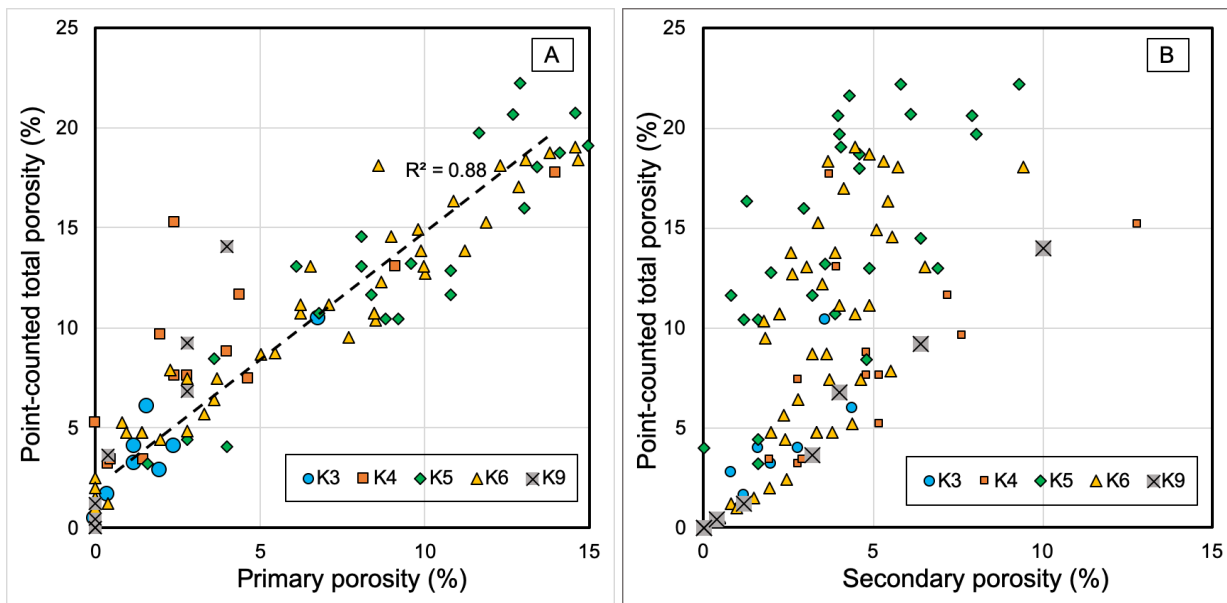


263



264

265 Figure 12. SEM micrograph of anhedral quartz cement (A) with irregular form in a sandstone from
 266 the crestal well K5 (TVD 4158 m, point-counted porosity 11.6%), and for comparison, euhedral
 267 quartz cement (B) from well K9 (TVD 4404m, point-counted porosity 14%). Microporosity can
 268 be seen between individual anhedral quartz cement crystals. The space is likely filled by petroleum
 269 that stops the quartz cement from forming euhedral crystal faces. This irregular quartz morphology
 270 could be a diagnostic feature for petroleum emplacement inhibiting quartz cementation.



271

272 Figure 13. Plots of primary porosity (A) and secondary porosity (B) versus total porosity (point-
273 counted) in the Kessog Sandstone. The porosity in the high-porosity sandstones is pre-dominantly
274 primary in origin.

275 **DISCUSSION**

276 **Possible cause of high porosity**

277 How does a sandstone retain high porosity during deep burial? Or what kind of sandstone
278 retains porosity at depth? One of the most critical factors in deciding the porosity of a sandstone
279 during burial is its depositional composition and texture (Bjørlykke and Jahren, 2015). For
280 example, clean, fine-grained and well-sorted sandstones are more likely to become high-porosity
281 reservoirs at depth since the rocks can develop a robust texture to resist mechanical compaction
282 (Chuhan et al., 2003). Besides this, there are five other commonly invoked mechanisms to explain
283 the occurrence of high-porosity sandstone reservoirs: grain-coating microquartz (Aase et al., 1996;
284 Aase and Walderhaug, 2005; Jahren and Ramm, 2000) and chlorite (Ajdukiewicz and Larese,
285 2012; Dowey et al., 2012; Ehrenberg, 1993); porefluid overpressure (Osborne and Swarbrick,
286 1999; Stricker and Jones, 2016); mineral dissolution (i.e. secondary porosity; Day-Stirrat et al.,
287 2010; Wilkinson et al., 2003) and early petroleum emplacement. In addition, bitumen coats on
288 quartz grains (Maast et al., 2011), phosphate poisoning of mineral surfaces (Warren and Pulham,
289 2001) and thermal anomalies near salt (Taylor et al., 2010), which are relatively less common, are
290 also potential mechanisms. This section assesses which of the mechanisms is responsible for high
291 porosity in the Kessog Field.

292 **Grain-size, sorting and mineralogy:** petrographic data show little difference in grain size
293 and sorting between different wells of the Kessog Field (Table 2). The high-porosity sandstones
294 of well K5 do not show any depositional texture that could account for the high porosity. In

295 addition, sandstones with a similar texture as the high-porosity sandstones are generally more
296 quartz-cemented in the other wells, e.g. in Figure 9. This suggests that a similar depositional
297 texture can equally form a high- or low-porosity sandstone in different parts of the same oilfield
298 reservoir (**Error! Reference source not found.**Figure 9).

299 The high-porosity sandstones of well K5 also show similar mineralogical composition as
300 the other sandstones (Table 2). The only noteworthy difference is the volume of illite. Illite is a
301 key mineral that can affect compaction and therefore the porosity of a sandstone, as a high content
302 of detrital illite present as clasts may significantly enhance sandstone compaction (Chuhan et al.,
303 2003). Point-count results show that sandstones of well K5 contain less illite than the sandstones
304 of wells K4, K6 and K9 (Table 2), indicating that the lesser volume illite may contribute to the
305 porosity preservation in well K5. However, this scenario can be refuted by the mineralogy and
306 porosity data from well K3, which contains even less illite than well K5 but the porosity is
307 comparable to the regional norm (Figure 2). Hence, there is no evidence to support that variation
308 in any mineralogical component as the cause of high-porosity in the Kessog Field.

309 **Grain coats:** grain-coating micro-quartz that is capable of preserving sandstone porosity by
310 inhibiting quartz cementation occurs in sandstones of marine origin (Aase and Walderhaug, 2005).
311 This is because the micro-quartz is precipitated from the dissolution of detrital siliceous sponge
312 spicules (Aase et al., 1996; Worden et al., 2012). Nonetheless, there have been few exceptional
313 cases in which micro-quartz grows in fluvial-deltaic sandstones: the examples include the fluvial
314 Skagerrak Formation in the North Sea (Nguyen et al., 2013), and the Safaniya Sandstone in Saudi
315 Arabia (Çağatay et al., 1996). The micro-quartz cement in these sandstones was interpreted as
316 being precipitated from silica-saturated fluvial waters and occurs only in trace amount that is
317 insufficient to reduce quartz cementation. The Pentland Formation was deposited in a fluvial-

318 deltaic setting; as such, micro-quartz cement is not expected to occur. In practice, micro-quartz
319 cement has not been observed in any sandstone samples from the Pentland Formation under the
320 optical microscope or SEM.

321 As for chlorite coats, previous studies on the petrology and mineralogy of the Pentland
322 Formation have not reported any chloritic clays or grain-coats in the sandstones (Coward, 2003;
323 Wilkinson et al., 2014). In the Kessog Field in particular, optical and scanning electron microscopy
324 in this study has not observed any chlorite grain coats in the reservoir sandstones, which eliminates
325 the possibility that chlorite coats are preserving sandstone porosity.

326 Grain-rimming or coating illite, however, is common in the sandstones. But the effectiveness
327 of illite coats inhibiting quartz cementation is uncertain: on the one hand, only a few studies (e.g.
328 Heald and Larese, 1974; Storvoll et al., 2002) have asserted that sandstones with illite coats have
329 low quartz cement and high porosity; on the other hand, many more studies have indicated that
330 illite coats have enhanced pressure solution between quartz grains, causing more porosity loss (e.g.
331 Bjørkum, 1996; Oelkers et al., 1996; Thomson and Stancliffe, 1990; Walderhaug, 1994). In the
332 case of the Kessog Field, quartz cement is not observed on the surface of quartz grains that are
333 covered by thick illite coats ($>10\ \mu\text{m}$, e.g. in Figure 10A), suggesting the coats may have inhibited
334 quartz cementation. However, thin grain coats ($<10\ \mu\text{m}$), such as the illite rims in Figure 10B, are
335 commonly overgrown by quartz cement and do not appear to inhibit quartz cementation. Thick
336 illite coats in the Kessog sandstones are only present on a limited number of quartz grains (Figure
337 10A) and therefore, their effectiveness in inhibiting quartz cementation for the whole reservoir is
338 considered to be negligible. Also, the high-porosity sandstones of well K5 were observed to
339 contain no more illite coats than the other sandstones, which disproves the hypothesis of illite coats
340 preserving porosity in the sandstones.

341 **Overpressure:** all the Pentland Formation reservoirs are overpressured to similar degrees
342 below a depth of 4.2 km (Figure 8), hence the effect of overpressure on the compaction of
343 sandstone is expected to be similar for all these reservoirs. Overpressure therefore cannot account
344 for the observed porosity difference between different Pentland wells or oilfields.

345 **Secondary porosity:** in the high-porosity sandstones of well K5, the point-count results show
346 that the type of porosity is dominated by primary porosity (Table 2). In comparison, the amount
347 of secondary porosity in the high-porosity sandstones of well K5 is not significantly higher than
348 in the sandstones of wells K3, K4, K6 and K9 (Table 2, Figure 13). This suggests that the high
349 porosity was formed through the preservation of primary porosity, rather than the creation of
350 porosity by grain dissolution.

351 **Other potential mechanisms:** Maast et al. (2011) noticed a highly porous section of
352 sandstones between the oil-leg and water-leg of the reservoir of the Miller Field, UK Central North
353 Sea (well 16/3b-5). This section of sandstones is about 15m thick, containing porosity that is
354 approximately 10% higher than both the oil- and water-legs of the reservoir. Through observations
355 under the microscope, Maast et al. (2011) concluded that this high porosity is preserved by grain-
356 coating bitumens on quartz grains. The high porosity sandstones in the Kessog Field, however,
357 mostly occur in the top of the reservoir where it is petroleum saturated. This is not where bitumen
358 would be expected to form. Two other mechanisms — phosphate poisoning of grain surfaces
359 (Warren and Pulham, 2001) and thermal anomalies near salt (Taylor et al., 2010) are unlikely to
360 happen in the Kessog Field as it is not close to any known phosphate or salt beds.

361

362 **Influence of petroleum on the sandstone porosity**

363 If the porosity of a reservoir is preserved by petroleum emplacement, what porosity
364 distribution pattern is expected? Since petroleum is less dense than water, it would first accumulate
365 in the top of a reservoir and then gradually fill toward the bottom. Therefore, if petroleum is
366 capable of preserving sandstone porosity, porosity preservation is expected to be the greatest at the
367 reservoir top, and to decrease downwards, as the time of petroleum emplacement becomes later
368 (Wilkinson and Haszeldine, 2011). This is consistent with the pattern of porosity variation within
369 the Kessog Field, where the highest porosity occurs in the shallowest well K5 (Table 1); the
370 reservoir porosity in the well is 9 – 11 % higher than the porosity of the other wells (Table 1).
371 Also, quartz cement in well K5 is significantly less abundant (2 – 5 % less) than in the other wells
372 (Figure 11, Table 2). Hence, the variations of porosity and quartz cement within the reservoir of
373 the Kessog Field can be well explained by the process of petroleum emplacement.

374 The grain contacts in the high-porosity sandstones of well K5 are typically long-contacts
375 (Figure 10A); combined with the small volume of quartz cement (2-3%), it can be inferred that the
376 petrography of the high-porosity sandstones is similar to a sandstone that is buried to only 2-3 km
377 (80 – 115°C) in the North Sea Basin. This is supported by experimental sandstone compaction
378 curves and empirical oilfield data (Gluyas and Cade, 1997), which suggest that the porosity of
379 well K5's sandstone (25%) normally occurs in sandstones buried at approximately 2.5 km in the
380 North Sea, giving an estimate of the depth of petroleum emplacement. The small volume (2-3%)
381 of quartz cement in the sandstone can effectively retard or prevent significant porosity loss by
382 compaction (McBride, 1989), but further growth of quartz cement has been inhibited by petroleum
383 emplacement. This would result in a sandstone reservoir whose porosity can be preserved to
384 greater depth, and one petrographic feature of these sandstones influenced by early petroleum

385 emplacement is that primary porosity dominates over secondary porosity, as is observed in the
386 sandstones of well K5 (Table 2).

387

388 **Petroleum emplacement retarding K-feldspar dissolution**

389 Another feature of the high-porosity sandstones in well K5 is the significantly higher amount
390 of K-feldspar than the other sandstones (Figure 11, Table 2); meanwhile, kaolin, which is a product
391 of K-feldspar dissolution (Bjørlykke and Jahren, 2015; Yuan et al., 2019), is scarce (0.7 ± 0.2 %).
392 There are three possible mechanisms that can potentially cause the variation of K-feldspar and
393 kaolin within the Kessog Field.

394 Firstly, K-feldspar and kaolin could be controlled by variations in the original sandstone
395 composition. However, as previously discussed, the petrographic data show otherwise uniform
396 sandstone composition and texture across the field. And if the K5 sandstones were richer in K-
397 feldspar upon deposition, then the lack of diagenetic kaolin becomes problematic. Therefore,
398 variation in detrital composition is not a reasonable explanation for the high content of K-feldspar
399 but less abundant kaolin in well K5.

400 The second possible explanation is that the pattern of K-feldspar and kaolin was controlled
401 by meteoric water flushing when the sandstones were close to the paleo-ground surface. The
402 presence of the unconformity surface at the top of the Kessog Reservoir indicates the sandstones
403 had been subjected to sub-aerial erosion in the past (Figure 5). The K5 sandstones are much thinner
404 (23.5 m) than the sandstones of the other wells, which are all greater than 100 m thick (Table 1).
405 This suggests that the well K5 has been subjected to more erosion, and correspondingly more
406 meteoric water flux, than the latter, so that greater transformation of K-feldspar to kaolin might be

407 expected here. As this is the opposite of the observed pattern, this refutes the hypothesis that the
408 preservation of K-feldspar in well K5 is because of less meteoric water leaching near the surface.

409 The third possible scenario is that K-feldspar dissolution in well K5 was inhibited by
410 petroleum emplacement in a manner analogous to petroleum restricting silica mobility (Worden et
411 al., 1998). The emplacement of petroleum limits the transport of the ions released by K-feldspar
412 dissolution, thereby impeding K-feldspar dissolution and the growth of kaolin. Overall, petroleum
413 emplacement inhibiting K-feldspar dissolution is the most reasonable explanation for the
414 preservation of K-feldspar in the K5 sandstones.

415

416 **Implication for petroleum reservoir quality prediction**

417 This study delivers a clear answer to the controversial question of whether petroleum
418 emplacement can preserve sandstone porosity in diagenesis. The quartz arenite reservoir of the
419 Kessog Field with high oil saturations is shown to contain up to 11% higher porosity than the
420 otherwise similar water-saturated sandstones (Figure 2). Petroleum emplacement inhibiting quartz
421 cementation is concluded to be the primary cause of the high porosity. This effect of porosity
422 preservation by petroleum emplacement is important for exploration ventures targeted on deep oil
423 and gas reservoirs, which may be previously deemed uneconomic due to predicted low porosity
424 and permeability. Conventional reservoir quality prediction models forecast significant reservoir
425 quality risk with these targets as they are under elevated temperature and pressure conditions and
426 possibly subjected to extensive quartz cementation and a high degree of compaction (Lander et al.,
427 2008; Walderhaug, 2000). However, if these reservoirs had been charged with petroleum in the
428 early stages of diagenesis, prior to the onset of quartz cementation, primary porosity in these
429 reservoirs might be significantly preserved during deep burial. Basin modelling identifying

430 reservoirs with early petroleum emplacement can be a useful tool for screening and designating
431 the potential deep reservoirs of high porosity. Also, reservoir models aiming at predicting quartz
432 cement and reservoir quality in sandstones should take into account the timing and rate of
433 petroleum emplacement to produce a more accurate modelling result.

434 This work also suggests that petroleum emplacement in the Kessog Field has hindered the
435 process of K-feldspar dissolution to precipitate kaolin in the sandstone reservoir. Since all
436 diagenetic chemical reactions take place through an aqueous phase, it is reasonable to speculate
437 that petroleum emplacement can also affect many other diagenetic reactions due to the disruption
438 of chemical ions' transport pathways between reactants and precipitation sites after petroleum
439 emplacement. Processes such as illitization of smectite and carbonate cementation, which have
440 profound influence on sandstone reservoir quality (Giles and de Boer, 1990; Morad, 1998), may
441 also be influenced by petroleum emplacement process. There is, however, only limited published
442 work concerning the effect of petroleum emplacement on clay mineral diagenesis (e.g. Midtbø et
443 al., 2000; Worden and Barclay, 2003) or carbonate cementation (e.g. Lei et al., 2019). Particularly,
444 the relationship between petroleum emplacement and various diagenetic reactions in sandstones
445 needs to be further considered and explored in future studies. Progress can be made with examining
446 reservoirs with limited facies variation, in conjunction with high-quality petrographic data and
447 fluid saturation analysis.

448

449 **CONCLUSION**

450 1. Sandstones of the Kessog Field have higher porosity than expected from regional trends. The
451 average porosity of crestal well K5 is 25%, which is 11% higher than the porosity (14%)
452 predicted for the Pentland Sandstone at the corresponding depth; the porosity of a few

453 sandstones in wells K3, K4, K6 and K9 are also exceptional, ranging between 15% and 30%.
454 The majority of these high-porosity sandstones are saturated with oil (>40%).

455 2. Grain-size, sorting and mineralogy of the high-porosity sandstones are similar to the medium-
456 to low porosity sandstones, suggesting the original sandstone composition and texture do not
457 account for the occurrence of high porosity. The impact of grain-coats (microquartz, chlorite
458 and illite), reservoir overpressure and mineral dissolution on the porosity of the Kessog
459 reservoir can be shown to be insignificant. Petroleum emplacement inhibiting quartz
460 cementation is the only possible mechanism that can explain the occurrence of high-porosity
461 in the Kessog Field.

462 3. The high-porosity sandstones under the influence of petroleum emplacement exhibit four
463 characteristics: (1) they occur at the crest of the reservoir; (2) primary porosity is the main
464 type of porosity; (3) there is 2 - 5% less quartz cement than the water-saturated sandstones;
465 (4) there are 2 - 3% more K-feldspar and 2 - 6% less kaolin than the water-saturated sandstone,
466 indicating that petroleum emplacement has also inhibited K-feldspar dissolution.

467

468 **ACKNOWLEDGEMENTS**

469 We would like to gratefully acknowledge Richard H. Worden (University of Liverpool) and
470 Rachel A. Wood (University of Edinburgh) for their useful comments on this work. The British
471 Geological Survey and BP are thanked for kindly providing the study samples. The China
472 Scholarship Council is acknowledged for sponsoring Xia's doctoral study. Schlumberger kindly
473 donated PetroMod™ licenses.

474 This research did not receive any specific grant from funding agencies in the public,
475 commercial, or not-for-profit sectors.

476

477 **REFERENCE**

478 Aase, N.E., Bjørkum, P.A., Nadeau, P.H., 1996. The effect of grain-coating
479 microquartz on preservation of reservoir porosity. *Am. Assoc. Pet. Geol. Bull.* 80, 1654–
480 1673. <https://doi.org/10.1306/64EDA0F0-1724-11D7-8645000102C1865D>

481 Aase, N.E., Walderhaug, O., 2005. The effect of hydrocarbons on quartz cementation:
482 diagenesis in the Upper Jurassic sandstones of the Miller Field, North Sea, revisited. *Pet.*
483 *Geosci.* 11, 215–223. <https://doi.org/10.1144/1354-079304-648>

484 Ajdukiewicz, J.M., Larese, R.E., 2012. How clay grain coats inhibit quartz cement and
485 preserve porosity in deeply buried sandstones: Observations and experiments. *Am. Assoc.*
486 *Pet. Geol. Bull.* 96, 2091–2119. <https://doi.org/10.1306/02211211075>

487 Barclay, S.A., Worden, R.H., 1998. Quartz cement volumes across oil-water contacts in oil
488 fields from petrography and wireline logs: preliminary results from the Magnus Field, Northern
489 North Sea, in: Harvey, P.K., Lovell, M.A. (Eds.), *Core-Log Integration*. Geol. Soc. London, Spec.
490 Publ. 136, 327–339. <https://doi.org/10.1144/GSL.SP.1998.136.01.27>

491 Bjørkum, P.A., 1996. How important is pressure in causing dissolution of quartz in
492 sandstones? *J. Sediment. Res.* 66, 147–154. [https://doi.org/10.1306/D42682DE-2B26-](https://doi.org/10.1306/D42682DE-2B26-11D7-8648000102C1865D)
493 [11D7-8648000102C1865D](https://doi.org/10.1306/D42682DE-2B26-11D7-8648000102C1865D)

494 Bjørlykke, K., Jahren, J., 2015. Sandstones and Sandstone Reservoirs, in: *Petroleum*
495 *Geoscience: From Sedimentary Environments to Rock Physics*, Second Edition. pp. 119–
496 149. <https://doi.org/10.1007/978-3-642-34132-8>

497 Bloch, S., Lander, R.H., Bonnell, L., 2002. Anomalously high porosity and
498 permeability in deeply buried sandstone reservoirs: Origin and predictability. *Am. Assoc.*

499 Pet. Geol. Bull. 86, 301–328. <https://doi.org/10.1306/61EEDABC-173E-11D7->
500 8645000102C1865D

501 Çağatay, N.M., Saner, S., Al-Saiyed, I., Carrigan, W.J., 1996. Diagenesis of the
502 Safaniya Sandstone Member (mid-Cretaceous) in Saudi Arabia. *Sedimentary Geol.* 105,
503 221-239. [https://doi.org/10.1016/0037-0738\(95\)00140-9](https://doi.org/10.1016/0037-0738(95)00140-9)

504 Chuhan, F.A., Kjeldstad, A., Bjørlykke, K., Høeg, K., 2003. Experimental compression
505 of loose sands: relevance to porosity reduction during burial in sedimentary basins. *Can.*
506 *Geotech. J.* 40, 995–1011. <https://doi.org/10.1139/t03-050>

507 Clark, D.N., Riley, L.A., Ainsworth, N.R., 1993. Stratigraphic, structural and
508 depositional history of the Jurassic in the Fisher Bank Basin, UK North Sea, in: Parker, J.R.
509 (Ed.) *Petroleum Geology of Northwest Europe: Proceedings of the 4th Conference.* Geol.
510 Soc. London, pp. 415–424. <https://doi.org/10.1144/0040415>

511 Coward, R.N., 2003. The Erskine Field, Block 23/26, UK North Sea. in: Gluyas, J. G.,
512 Hichens, H. M. (Eds.) *United Kingdom Oil and Gas Fields Commemorative Millennium*
513 *Volume.* Geol. Soc. London, Mem. 20, pp. 523–535.
514 <https://doi.org/10.1144/GSL.MEM.2003.020.01.42>

515 Day-Stirrat, R.J., Milliken, K.L., Dutton, S.P., Loucks, R.G., Hillier, S., Aplin, A.C.,
516 Schleicher, A.M., 2010. Open-system chemical behavior in deep Wilcox Group mudstones,
517 Texas Gulf Coast, USA. *Mar. Pet. Geol.* 27, 1804–1818.
518 <https://doi.org/10.1016/j.marpetgeo.2010.08.006>

519 Deegan, C.E., Scull, B.J., 1977. A standard lithostratigraphic nomenclature for the
520 Central and Northern North Sea. HMSO, London. ISBN 0118840185.

521 Dowey, P.J., Hodgson, D.M., Worden, R.H., 2012. Pre-requisites, processes, and
522 prediction of chlorite grain coatings in petroleum reservoirs: A review of subsurface
523 examples. *Mar. Pet. Geol.* 32, 63–75. <https://doi.org/10.1016/j.marpetgeo.2011.11.007>

524 Ehrenberg, S.N., 1993. Preservation of anomalously high porosity in deeply buried
525 sandstones by grain-coating chlorite: Examples from the Norwegian continental shelf.
526 *Amer. Ass. Pet. Geol. Bull.* 77, 1260–1286.

527 Eriksen, S.H., Anderson, J.H., Grist, M., Stoker, S., Brzozowska, J., 2003. Oil and gas
528 resources, in: Evans, D., Graham, C., Armour, A., Bathurst, P. (Eds.), *The Millennium*
529 *Atlas: Petroleum Geology of the Central and Northern North Sea*. The Geological Society
530 of London, London, pp. 345–358.

531 Folk, R.R.L., 1974. *Petrology of sedimentary rocks*, 2nd edition. Hemphill Publishing
532 Company, Austin, TX. <http://hdl.handle.net/2152/22930>

533 Giles, M.R., de Boer, R.B., 1990. Origin and significance of redistributive secondary
534 porosity. *Mar. Pet. Geol.* 7, 378–397. [https://doi.org/10.1016/0264-8172\(90\)90016-A](https://doi.org/10.1016/0264-8172(90)90016-A)

535 Giles, M.R., Stevenson, S., Martin, S. V, Cannon, S.J.C., Hamilton, P.J., Marshall,
536 J.D., Samways, G.M., 1992. The reservoir properties and diagenesis of the Brent Group: a
537 regional perspective, in: Morton, A.C., Haszeldine, R.S., M. R. Giles, Brown, S. (Eds.)
538 *Geology of the Brent Group*. *Geol. Soc. London, Spec. Publ.* 61, pp. 289–327.
539 <https://doi.org/10.1144/GSL.SP.1992.061.01.16>

540 Gluyas, J., Cade, C., 1997. Prediction of Porosity in Compacted Sands, in: Kupecz, J. A.,
541 Gluyas, J., Bloch, S. (Eds.) *Reservoir Quality Prediction in Sandstones and Carbonates*.
542 AAPG Mem. 69, pp. 19–28. DOI: <https://doi.org/10.1306/M69613>

543 Gluyas, J., Hitchens, H., 2003. United Kingdom oil and gas fields: commemorative
544 millennium volume, Geol. Soc. London, Mem. 20.

545 Gluyas, J.G., Robinson, G., Emery, D., Grant, S.M., Oxtoby, N.H., 1993. The link
546 between petroleum emplacement and sandstone cementation, in: Parker J. R. (Ed.) Proc. 4th
547 Conference Petroleum Geology of Northwest Europe 2. Geol. Soc., London, pp. 1395–
548 1404. <https://doi.org/10.1144/0041395>

549 Heald, M.T., Larese, R.E., 1974. Influence of coatings on quartz cementation. J.
550 Sediment. Petrol. 44, 1269–1274. [https://doi.org/10.1306/212F6C94-2B24-11D7-
551 8648000102C1865D](https://doi.org/10.1306/212F6C94-2B24-11D7-8648000102C1865D)

552 Jahren, J., Ramm, M., 2000. The Porosity-Preserving Effects of Microcrystalline
553 Quartz Coatings in Arenitic Sandstones: Examples from the Norwegian Continental Shelf,
554 in: Worden, R.H., Morad, S. (Eds.) Quartz Cementation in Sandstones. Wiley, pp. 271–280.
555 <https://doi.org/10.1002/9781444304237.ch18>

556 Kong, M., Bhattacharya, R.N., James, C., Basu, A., 2005. A statistical approach to
557 estimate the 3D size distribution of spheres from 2D size distributions. Geol. Soc. Am. Bull.
558 117, 244. <https://doi.org/10.1130/B25000.1>

559 Lander, R.H., Larese, R.E., Bonnell, L.M., 2008. Toward more accurate quartz cement
560 models: The importance of euhedral versus noneuhedral growth rates. Am. Assoc. Pet.
561 Geol. Bull. 92, 1537–1563. <https://doi.org/10.1306/07160808037>

562 Lei, Z., Xu, H., Liu, Q., Li, W., Yan, D., Li, S., Lei, P., Yan, M., Li, J., 2019. The
563 influence of multiple-stage oil emplacement on deeply buried marine sandstone diagenesis:
564 A case study on the Devonian Donghe sandstones, Tabei Uplift, Tarim Basin, NW China.
565 Mar. Pet. Geol. 110, 299–316. <https://doi.org/10.1016/J.MARPETGEO.2019.07.030>

566 Maast, T.E., Jahren, J., Bjørlykke, K., 2011. Diagenetic controls on reservoir quality in
567 middle to upper Jurassic sandstones in the South Viking Graben, North Sea. *Am. Assoc.*
568 *Pet. Geol. Bull.* 95, 1937–1958. <https://doi.org/10.1306/03071110122>

569 Marchand, A.M.E., Haszeldine, R.S., Smalley, P.C., Macaulay, C.I., Fallick, A.E.,
570 2001. Evidence for reduced quartz-cementation rates in oil-filled sandstones. *Geology* 29,
571 915–918. [https://doi.org/10.1130/0091-7613\(2001\)029<0915:EFRQCR>2.0.CO;2](https://doi.org/10.1130/0091-7613(2001)029<0915:EFRQCR>2.0.CO;2)

572 McBride, E.F., 1989. Quartz cement in sandstones: a review. *Earth-Science Rev.* 26,
573 69–112. [https://doi.org/10.1016/0012-8252\(89\)90019-6](https://doi.org/10.1016/0012-8252(89)90019-6)

574 McManus, J., 1988. Grain size determination and interpretation, in: Tucker, M. (Ed.),
575 *Techniques in Sedimentology*. Blackwell Scientific Publications, pp. 63–85.

576 Midtbø, R.E.A., Rykkje, J.M., Ramm, M., 2000. Deep burial diagenesis and reservoir
577 quality along the eastern flank of the Viking Graben. Evidence for illitization and quartz
578 cementation after hydrocarbon emplacement. *Clay Miner.* 35, 227–237.
579 <https://doi.org/10.1180/000985500546602>

580 Molenaar, N., Cyziene, J., Sliupa, S., Craven, J., 2008. Lack of inhibiting effect of oil
581 emplacement on quartz cementation: Evidence from Cambrian reservoir sandstones,
582 Paleozoic Baltic Basin. *Geol. Soc. Am. Bull.* 120, 1280–1295.
583 <https://doi.org/10.1130/B25979.1>

584 Morad, S., 1998. *Carbonate Cementation in Sandstones: Distribution Patterns and*
585 *Geochemical Evolution*. IAS Special Publication, 26, Wiley. DOI:10.1002/9781444304893

586 Moss, B., Barson, D., Rakhit K., Dennis, H., 2003. Formation pore pressures and
587 formation waters, in: Evans, D., Graham, C., Armour, A., Bathurst, P. (Eds.). *Millennium*

588 Atlas: Petroleum Geology of the Central and Northern North Sea. Millennium Atlas Co.
589 Ltd., pp. 317–329.

590 Nguyen, B.T.T., Jones, S.J. Goult, N.R. Middleton, A.J., Grant, N., Ferguson, A.
591 Bowen, L., 2013. The role of fluid pressure and diagenetic cements for porosity
592 preservation in Triassic fluvial reservoirs of the Central Graben, North Sea. *Amer. Ass. Pet.*
593 *Geol. Bull.* 97, 1273–1302. <https://doi.org/10.1306/01151311163>

594 Oelkers, E.H., Bjorkum, P.A., Murphy, W.M., 1996. A petrographic and
595 computational investigation of quartz cementation and porosity reduction in North Sea
596 sandstones. *Am. J. Sci.* 296, 420–452. <https://doi.org/10.2475/ajs.296.4.420>

597 Offshore Europe, 2001. Offshore Europe [WWW Document]. URL
598 [http://www.offshore-mag.com/articles/print/volume-61/issue-2/departments/offshore-](http://www.offshore-mag.com/articles/print/volume-61/issue-2/departments/offshore-europe.html)
599 [europe.html](http://www.offshore-mag.com/articles/print/volume-61/issue-2/departments/offshore-europe.html) (accessed 2.7.18).

600 Osborne, M.J., Swarbrick, R.E., 1999. Diagenesis in North Sea HPHT clastic
601 reservoirs — consequences for porosity and overpressure prediction. *Mar. Pet. Geol.* 16,
602 337–353. [https://doi.org/10.1016/S0264-8172\(98\)00043-9](https://doi.org/10.1016/S0264-8172(98)00043-9)

603 Oye, O.J., Aplin, A.C., Jones, S.J., Gluyas, J.G., Bowen, L., Orland, I.J., Valley, J.W.,
604 2018. Vertical effective stress as a control on quartz cementation in sandstones. *Mar. Pet.*
605 *Geol.* 98, 640–652. <https://doi.org/10.1016/j.marpetgeo.2018.09.017>

606 Richards, P.C., Lott, G.K., Johnson, H., Knox, R.W., 1993. Jurassic of the central and
607 northern North Sea. *Lithostratigraphic Nomenclature UK North Sea*, 3, UK Offshore
608 Operators Association. ISBN 0 85272 212 5.

609 Storvoll, V., Bjørlykke, K., Karlsen, D., Saigal, G., 2002. Porosity preservation in
610 reservoir sandstones due to grain-coating illite: A study of the Jurassic Garn Formation

611 from the Kristin and Lavrans fields, offshore Mid-Norway. *Mar. Pet. Geol.* 19, 767–781.
612 [https://doi.org/10.1016/S0264-8172\(02\)00035-1](https://doi.org/10.1016/S0264-8172(02)00035-1)

613 Stricker, S., Jones, S.J., 2016. Enhanced porosity preservation by pore fluid
614 overpressure and chlorite grain coatings in the Triassic Skagerrak, Central Graben, North
615 Sea, UK, in: Armitage, P.J., Butcher, A.R., Churchill, J.M., Csoma, A.E., Hollis, C.,
616 Lander, R.E., Omma, J.E., Worden, R.H. (Eds.) *Reservoir Quality of Clastic and Carbonate*
617 *Rocks: Analysis, Modelling and Prediction*. Geol. Soc. London, Spec. Publ. 435, pp. 321-
618 341. <https://doi.org/10.1144/SP435.4>

619 Taylor, T., Giles, M., Hathon, L., Diggs, T., 2010. Sandstone diagenesis and reservoir
620 quality prediction: Models, myths, and reality. *Amer. Ass. Pet. Geol. Bull.* 94, 1093–1132.
621 <https://doi.org/10.1306/04211009123>

622 Thomson, A., Stancliffe, R.J., 1990. Diagenetic controls on reservoir quality, eolian Norphlet
623 Formation, South State Line Field, Mississippi, in: Barwis J.H., McPherson J.G., Studlick J.R.J.
624 (Eds.), *Sandstone Petroleum Reservoirs. Casebooks in Earth Sciences*. Springer, New York, NY.
625 pp. 205–224. DOI https://doi.org/10.1007/978-1-4613-8988-0_10

626
627 Walderhaug, O., 1994. Precipitation rates for quartz cement in sandstones determined by fluid
628 inclusion microthermometry and temperature-history modelling. *J. Sediment. Res.* 64A, 324–
629 333. <https://doi.org/10.2110/jsr.64.324>

630 Walderhaug, O., 2000. Modeling quartz cementation and porosity in Middle Jurassic
631 Brent Group sandstones of the Kvitebjorn field, Northern North Sea. *Am. Assoc. Pet. Geol.*
632 *Bull.* 84, 1325–1339. <https://doi.org/10.1306/A9673E96-1738-11D7-8645000102C1865D>

633 Warren, E.A., Pulham, A.J., 2001. Anomalous Porosity and Permeability Preservation
634 in Deeply Buried Tertiary and Mesozoic Sandstones in the Cusiana Field, Llanos Foothills,
635 Colombia. *J. Sediment. Res.* 71, 2–14. <https://doi.org/10.1306/081799710002>

636 Wilkinson, M., Haszeldine, R.S., 2011. Oil charge preserves exceptional porosity in
637 deeply buried, overpressured, sandstones: Central North Sea, UK. *J. Geol. Soc. London.*
638 168, 1285–1295. <https://doi.org/10.1144/0016-76492011-007>

639 Wilkinson, M., Haszeldine, R.S., Milliken, K.L., 2003. Cross-Formational Flux of
640 Aluminium and Potassium in Gulf Coast (USA) Sediments, in: Worden, R., Morad, S.
641 (Eds.), *Clay Cements in Sandstones*. IAS Special Publication, 34, pp. 147–160.
642 DOI:10.1002/9781444304336

643 Wilkinson, M., Haszeldine, R.S., Morton, A., Fallick, A.E., 2014. Deep burial
644 dissolution of K-feldspars in a fluvial sandstone, Pentland Formation, UK Central North
645 Sea. *J. Geol. Soc. London.* 171, 635–647. <https://doi.org/10.1144/jgs2013-144>

646 Worden, R., Barclay, S., 2003. The Effect of Oil Emplacement on Diagenetic Clay
647 Mineralogy: the Upper Jurassic Magnus Sandstone Member, North Sea, in: Worden, R.H.,
648 Morad, S. (Eds.), *Clay Mineral Cements in Sandstones*. IAS Special Publication, 34,
649 DOI:10.1002/9781444304336

650 Worden, R.H., Bukar, M., Shell, P., 2018. The effect of oil emplacement on quartz
651 cementation in a deeply buried sandstone reservoir. *Am. Assoc. Pet. Geol. Bull.* 102, 49–75.
652 <https://doi.org/10.1306/02071716001>

653 Worden, R.H., French, M.W., Mariani, E., 2012. Amorphous silica nanofilms result in
654 growth of misoriented microcrystalline quartz cement maintaining porosity in deeply buried
655 sandstones. *Geology* 40, 179–182. <https://doi.org/10.1130/G32661.1>

656 Worden, R.H., Oxtoby, N.H., Smalley, P.C., 1998. Can oil emplacement prevent
657 quartz cementation in sandstones? *Pet. Geosci.* 4, 129–137.

658 <https://doi.org/10.1144/petgeo.4.2.129>

659 Yuan, G., Cao, Y., Schulz, H.-M., Hao, F., Gluyas, J., Liu, K., Yang, T., Wang, Y., Xi,
660 K., Li, F., 2019. A review of feldspar alteration and its geological significance in

661 sedimentary basins: from shallow aquifers to deep hydrocarbon reservoirs. *Earth-Science*

662 *Rev.* 191, 114–140. <https://doi.org/10.1016/J.EARSCIREV.2019.02.004>

663